Biogeochemistry **51:** 113–140, 2000.

Methane emissions from the Orinoco River floodplain, Venezuela

LESLEY K. SMITH[1], WILLIAM M. LEWIS, JR.[1], JEFFREY P. CHANTON[2], GREG CRONIN[3] & STEPHEN K. HAMILTON[4]
[1]*Center for Limnology, Cooperative Institute for Research in Environmental Sciences, University of Colorado, Boulder, CO 80309-0216, U.S.A.;* [2]*Department of Oceanography, Florida State University, Tallahassee, FL 32306, U.S.A.;* [3]*Department of Biology, University of Colorado – Denver, Denver, CO 80217, U.S.A.;* [4]*Kellogg Biological Station, Michigan State University, 3700 E. Gull Lake Drive, Hickory Corners, MI 49060-9516, U.S.A.*

Key words: methane emissions, tropical floodplains, Orinoco River, floodplain forest, wetlands

Abstract. Methane emissions were measured over a 17-month interval at 21 locations on the Orinoco fringing floodplain and upper delta (total area, 14,000 km^2). Emissions totaled 0.17 Tg yr^{-1}, or 7.1 mmol d^{-1} (114 mg d^{-1}; standard deviation, ±18%) per m^2 of water surface. Ebullition accounted for 65% of emissions. Emission rates were about five times as high for floodplain forest as for open water or macrophyte mats. Emission rates were positively correlated with carbon content of sediment and amount of methane in the water column, and negatively correlated with dissolved oxygen, but the correlations were weak. Emission from floodplain soils occurred only when the water content of soil exceeded 25%, which occurred within 20 m of standing water during floodplain drainage (3 months/yr). Bare soils emitted 60 mmol/day per m of shoreline length; soils covered by stranded macrophyte beds emitted five times this amount. Total emissions were accounted for primarily by flooded forest (94%); macrophyte mats, open water, and exposed soils made only small contributions. The flux-weighted mean $\delta^{13}C$ for the floodplain was –62 ± 8‰; for δD the mean was –271 ± 27‰. The $\delta^{13}C$ and δD were negatively correlated. Overall emission rates were notably lower than for the Amazon. The depth and duration of flooding are considerably less for the Orinoco than for the Amazon floodplain; oxygen over sediments is the rule for the Orinoco but not for the Amazon. The Orinoco data illustrate the difficulty of generalizing emission rates. Current information for tropical America, including revised estimates for inundated area along the Amazon, indicate that methane emissions from tropical floodplains have been overestimated.

Introduction

Global sources of methane reaching the atmosphere are believed to include a large contribution from wetlands (ca. 25 percent: Matthews & Fung 1987, Cicerone & Oremland 1988). Tropical wetlands are considered especially important methane sources. For example, Bartlett and Harriss (1993) esti-

mated that wetlands lying between 20° north and 30° south latitude release about 66 Tg per year, or approximately 60% of the total emissions from natural wetlands.

Present estimates of methane emissions from tropical wetlands have three major weaknesses: (1) excessive dependence of global estimates on data from the Amazon, (2) insufficient information on seasonal and spatial variation of emissions, and (3) inadequate knowledge of wetland area in the tropics. The purpose of this paper is to contribute to the resolution of these deficiencies through the analysis of seasonal and spatial variation of emissions as well as an estimate of total methane emissions for the Orinoco River floodplain that can be compared with newly revised estimates for Amazonian emissions (Sippel et al. 1998; Melack & Forsberg, in press).

The Orinoco study includes measurements of stable isotope composition for methane emitted from the floodplain as well as a weighted estimate of isotopic composition for total emissions. Isotopic composition can be useful in evaluating mechanisms of methane production and the importance of methane oxidation (e.g. Whiticar et al. 1986; Happell et al. 1994), and in the construction of regional and global isotopic mass balances for atmospheric methane (e.g. Quay et al. 1991; Tyler 1991; Gupta et al. 1996).

The Orinoco River, which has the world's third largest discharge (38,000 m^3 s^{-1}, Lewis et al. 1995), inundates a fringing floodplain of approximately 6,500 km^2 and an adjoining deltaic floodplain of 20,000 km^2 (Hamilton & Lewis 1990a). The floodplain of the Orinoco differs from that of the Amazon, the origin of most measurements of tropical methane flux, in ways that may influence methane emission. The Orinoco floodplain has a more pronounced dry season (Hamilton & Lewis 1987; Lesack & Melack 1991) and, because the Orinoco floodplain is considerably shallower than the Amazon floodplain, its waters do not stratify or become anoxic over the sediments as readily (Hamilton & Lewis 1990b; Vásquez 1992; Melack & Fisher 1983; Tundisi et al. 1984).

The studies reported here include measurements of methane emissions along a 600-km reach of the Orinoco main stem and the upper delta between July 1991 and September 1992 (Figure 1). The measurements extended over the major aquatic habitat types on the floodplain and included floodplain soils that are alternately saturated and desiccated with the seasonal change in water level.

Study sites and sampling plan

Seasonal variation in rainfall causes a pronounced annual rise and fall of the Orinoco River (Figure 2). During the period of high water (July–December),

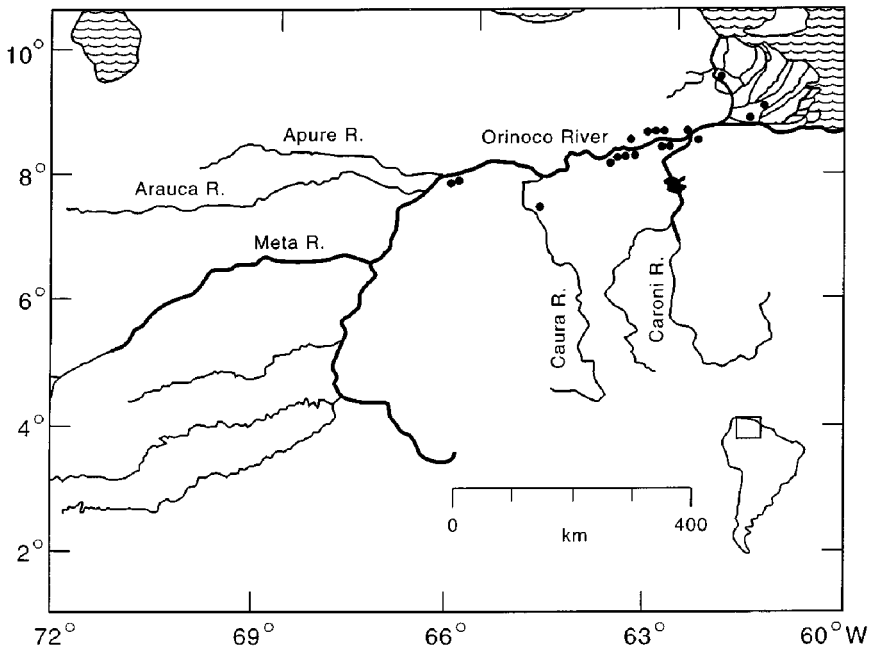

Figure 1. Location of the study area in Venezuela. Sampling locations are indicated by filled circles.

the river first fills, then flows through, and finally drains from the floodplain. These months of contact between the river and floodplain comprise the inundation season, during which phases of filling, throughflow, and drainage can be distinguished. Between January and June, the waters of the floodplain typically are not in contact with the river; this is the isolation season (seasons may vary two to four weeks from one year to the next). The water surface area of the floodplain changes progressively during both the inundation and isolation seasons; these changes in area must be accounted for in estimates of total methane emissions (as determined for present purposes by use of landsat data, aerial photography, and ground-based observations: Hamilton & Lewis 1990a). The water surface area expands during early inundation until it reaches its maximum extent in August and retains this extent into September, after which it contracts as the floodplain drains. During isolation, decline in surface area slows but continues as evaporation occurs in the absence of rainfall. Water surface area on the floodplain reaches its minimum extent in March, at the end of isolation, when the total area of standing water is about 6% of the maximum.

The fringing floodplain is composed of 2300 basins, each consisting of a central, uncanopied zone (floodplain lake) that includes open water and often

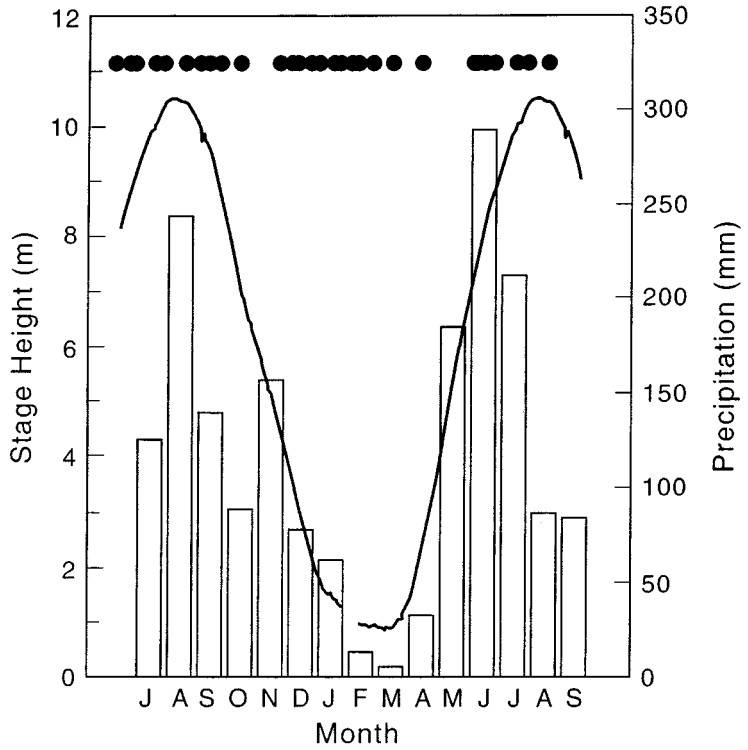

Figure 2. Hydrograph (solid line) of the lower Orinoco River just below its confluence with the Caroní River and annual precipitation (bars) for the years 1991 and 1992 (source: Palua Station, EDELCA, CVG Electrificatión del Caroní, C.A.). Sampling dates are indicated by the filled circles.

extensive macrophyte mats. The uncanopied zone is surrounded by floodplain forest. At maximum water level, 79% of the flooded area is forested, and at minimum water level the flooded area is restricted almost entirely to the open water zones of the floodplain lakes.

The deltaic portion of the floodplain lacks floodplain lakes. It consists primarily of forest, but macrophyte mats are also present. Small amounts of open water are found in the distributary channels through which the river water flows to the Caribbean (Van Andel 1967).

Waters of the fringing floodplain

Fifteen sites spanning 600 km on the fringing floodplain were chosen for repeated sampling (Figure 1). Each site was centered on a floodplain basin and included not only the uncanopied area of the basin (floodplain lake and macrophyte mats), but also the surrounding floodplain forest.

The fifteen sites were sampled on a rotational basis over 30 sampling dates between July 1991 and October 1992 (two sampling dates per site for the 15-month study). On any given date at a specific site, each of the three major habitat types (flooded forest, open water, macrophyte mats) was sampled at two or more locations, except when a given habitat type was absent. The sampling plan thus incorporated spatial variation within basins and among basins along the entire floodplain as well as temporal variation encompassing the annual cycle (Figure 2).

Sampling sites can be classified according to their water chemistry, the amounts of suspended solids that they receive from the river during inundation, the shapes of their lake basins, and the presence or absence of aquatic macrophytes. Fourteen of the sites are seasonally flooded by the Orinoco main stem, which carries a mixture of white water (water rich in suspended solids) from the Andes and the alluvial plain to the north of the Orinoco, and black water (water poor in suspended solids and highly colored by dissolved organic compounds) from the Guayana Shield to the south. One of the sites receives water only from the Caura River, a blackwater tributary of the Orinoco (Figure 1). Two of the lake basins are channel-shaped and 13 are dish-shaped. Ten of the lakes contained extensive macrophyte mats; the other 5 had few macrophytes.

Waters of the delta

Methane emissions were measured over a two-day period (July 1–2, 1991) at high water on the delta of the Orinoco River. The delta, which has an area of 22,500 km^2, is drained by nine major distributaries (van Andel 1967). The sampling sites, which included macrophyte mats as well as open water in three of the main channels (Manamo, Río Grande, and Araguao), were located on the upper delta (7500 km^2), where there is tidal influence but no saline water.

Habitat types on the delta (macrophytes, flooded forest) are also found on the fringing floodplain. For this reason, sampling on the delta was restricted to a single period during which the objective was to verify that habitat-specific rates of emission on the delta could be assumed similar to those measured on the fringing floodplain.

Floodplain soils

Emissions from soils were measured at Lake Mamo (8°26′00″ N, 63°07′00″ W) during October (inundation season, falling water phase) at intervals of about 10 m over two fixed 40-m transects that extended from the edge of the lake across the floodplain toward an escarpment that borders the floodplain

to the north of the river. These transects were resampled in May during the isolation season, by which time they were 500 m from the edge of the water.

Emissions from soils also were measured over 40-m transects at Lake Merecure (8°12′50″ N, 63°17′25″ W) during October and May. The transects at Lake Merecure were moved in concert with the shifting lake boundary so that their point of origin was always near the shoreline. At Lake Redonda (8°50′00″ N, 62°30′00″ W), emissions were measured within 20 m of the shoreline (median, 10 m) every two weeks between October 1991 and April 1992.

Methods

Methane emissions

Methane emissions were captured in floating chambers (Smith & Lewis 1992) that were deployed in duplicate at each sampling location. The chambers consisted of a lexan cube with an open bottom (L = 30 cm); these floated on the water with the aid of a small inflatable innertube located about 25 cm from the top of the chamber. For each deployment, depths of immersion were read at four locations around each chamber, and the headspace volume (ca. 16 L) was calculated from the four measurements. A reflective blanket was placed over three sides of the chamber, and light was allowed to penetrate the side of the chamber that was not facing the sun. Every 5 minutes for 20 minutes, duplicate gas samples were removed through a septum with a 5-cm^3 glass syringe equipped with a 3-way stopcock. Duplicate samples of ambient air were also collected before the chamber was deployed. The barrels of the syringes were filled with distilled water to minimize loss of gas after sampling.

Methane fluxes from exposed soils were measured in shaded aluminum chambers (L = 30 cm) with open bottoms and transparent lexan lids. The chambers were pushed 3–5 cm into the soil and were allowed to equilibrate for 30 minutes before they were sealed. Linearity of diffusion rates during the sampling interval indicated that the equilibration period was adequate. Four to eight randomly chosen locations were sampled along each transect on each sampling date.

Methane concentrations were measured within 24 hr of sampling with a portable gas chromatograph (GC) equipped with a packed column that was maintained at ambient temperature (25–30 °C). The methane standard (1793.6 ± 3.0 ppb) used for calibration was obtained from the Climate Monitoring and Diagnostic Laboratory of the National Oceanographic and Atmospheric Administration (Boulder, Colorado).

For samples over water, both diffusive and ebullitive fluxes were estimated. Diffusive fluxes were calculated from linear regression of concentration against time in the five samples that were collected over the 20-minute sampling interval. A regression corresponding to $p < 0.05$ was interpreted as indicating a quantifiable diffusive flux, the rate of which was estimated from the slope of the regression line. If the regression corresponded to $p > 0.05$, the data were examined. An abrupt increase in methane concentration was interpreted as ebullition, the amount of which was estimated as equal to the rise in concentration between samples bracketing the abrupt increase. If there was no abrupt increase, the ebullitive flux was assigned a value of zero, and the diffusive flux was deemed below the minimum for detection (ca. 0.16 mmol m^{-2} d^{-1}).

There was no significant difference between diffusive methane emissions from floating emergent macrophytes exposed to light (4.49 ± 3.36 mmol m^{-2} d^{-1}) and dark (4.86 ± 2.42 mmol m^{-2} d^{-1}) conditions within chambers (shrouded versus unshrouded chambers). Therefore, the diffusive methane emissions were measured between 0800 and 1600 and were assumed to be characteristic of the 24-hour mean rates. Wassmann et al. (1992) also found no diel variability in methane fluxes from floating aquatic macrophytes.

Other measurements

At flooded sites, water depth and profiles of water temperature (by thermistor), and dissolved oxygen by (polarographic sensor with stirrer) were measured on each sampling date. Water samples for dissolved methane were collected with a 60 cm^3 syringe immediately below the water surface or with a depth-selective sampler (Van Dorn bottle) at greater depths. The water samples were analyzed by gas chromatography after dissolved methane was stripped from the water with ambient air (Ioffe & Vitenberg 1984). Water samples also were collected on four occasions from the main stem of the Orinoco River near its confluence with the Caroní River for analysis of dissolved methane.

Soil and sediment characteristics

Surface sediments were collected with a sediment grab from 34 sites. Exposed soils were cored to a depth of 6 cm at four points along each transect. Coarse ($\geq$ 5 mm) organic material was removed, and the rest of the core was mixed for analysis. For both surface sediments and soil cores, three subsamples were weighed, dried to constant weight at 50 °C, and reweighed for determination of water content. The dried subsamples were ground and analyzed for total C and N by elemental analyzer.

Isotopic measurements

Methane from the three principal habitats at two sites (Lake Merecure and Lake Paso Acosta) was prepared for isotopic measurement as described by Chanton et al. (1992a). Methane was collected from air that was pumped from vented chamber head spaces into evacuated 4-L cylinders. Sedimentary methane, which potentially would have a different isotopic signature from that of atmospheric methane, was collected from gas bubbles that were released by the disturbance of sediments. The bubbles were collected in water-filled vials below the water surface. The vials were then sealed under water with butyl rubber stoppers. Because methane in gas bubbles from sediment is in equilibrium with methane of pore water, its isotopic composition is assumed to represent that of the sedimentary methane reservoir, as shown elsewhere (Martens et al. 1986; Chanton et al. 1992b).

Samples of methane were converted to CO_2 in a helium stream (50 mL min^{-1}) over copper oxide wire at 800 °C. A column of Schütze reagent was used to remove carbon monoxide. The presence of oxygen in canister or chamber samples does not affect the results of the combustion procedure; Chanton et al. (1992a) directly compared the combustion of bubble samples and pure methane standards diluted into air at low concentrations and found no difference in the results. Water resulting from the combustion of methane was converted to H_2 by reduction with zinc (Coleman et al. 1982). Purified CO_2 and H_2 samples were analyzed with an isotope ratio mass spectrometer. Stable isotope results are reported in the δ notation:

$$\delta‰ = (R_{\text{sample}}/R_{\text{std}} - 1) \times 1000$$

where R refers to the ratio of $^{13}C/^{12}C$ or D/H. The data reported here are referenced to PDB for C and SMOW for H (Hoefs 1987).

Results

Measurement variance

Replication of emission measurements (based on separate incubations within a few meters of each other over the same time interval) provides a basis for estimating measurement variance. In this case, the measurement variance includes natural microscale variation in the true emission rates as well as analytical and manipulation factors (subsampling with syringe, injection of sample into GC, etc.).

For diffusive fluxes, the standard deviation between replicates is linearly related to the emission rate ($p < 0.05$). The strong relationship between mean

and standard deviation suggests that the main source of variation is natural microscale patchiness in the environment rather than analytical error, which would be less dependent on emission rate. Because the relationship between mean and standard deviation is strongly linear, the ratio of the standard deviation to the mean can be estimated from the slope of a regression line relating mean and standard deviation, after the exclusion of samples for which the readings were below the detection limit. The slope of the regression line is 0.70, indicating that the coefficient of variation for individual measurements of diffusive flux made at a given site on a given date is 70%; the mean of duplicates at a given site would have a standard error of 50%.

Statistical analysis of replication variance for ebullition measurements is more difficult because most samples show no ebullition. Elimination of replicate pairs showing no ebullition in either replicate leaves a data set of $N = 42$ for analysis. Analysis of this data set by the same method that was applied to the diffusive fluxes shows that the variance increases with the mean, as expected, and that the standard deviation is linearly related to the emission rate ($p < 0.05$). The slope of the line indicates that the coefficient of variation for ebullition is 115% when ebullition occurs. For the mean of duplicate samples of which at least one shows occurrence of ebullition, the standard error is 81%.

The information on variance in measurements of ebullition and diffusion is used in estimating error in the final estimates of emission rates from the floodplain.

Characteristics of the pooled data

Methane emissions from aquatic habitats were measured a total of 412 times over the course of the study. The frequency distribution for total emissions (diffusive plus ebullitive fluxes) is shown in Figure 3. The distribution consists of two parts: (1) approximately one quarter of the measurements are not distinguishable from zero (including three slightly negative values), and (2) the positive emission rates show a unimodal distribution with a slight positive skew when plotted on a logarithmic scale.

Because ebullition and diffusion are not necessarily controlled by the same processes, their rates may not be correlated. A nonparametric test shows no significant relationship (Spearman rank correlation (r_s) = 0.16). There is a weak positive nonparametric correlation when the analysis is restricted to nonzero values ($r_s = 0.30$).

Figure 3 shows the frequency distribution of diffusive fluxes on a logarithmic scale. The form of the distribution is similar to that for total fluxes, except that there is less skew in the nonzero portion of the distribution because ebullition accounts for most of the very high rates, and diffusion accounts for

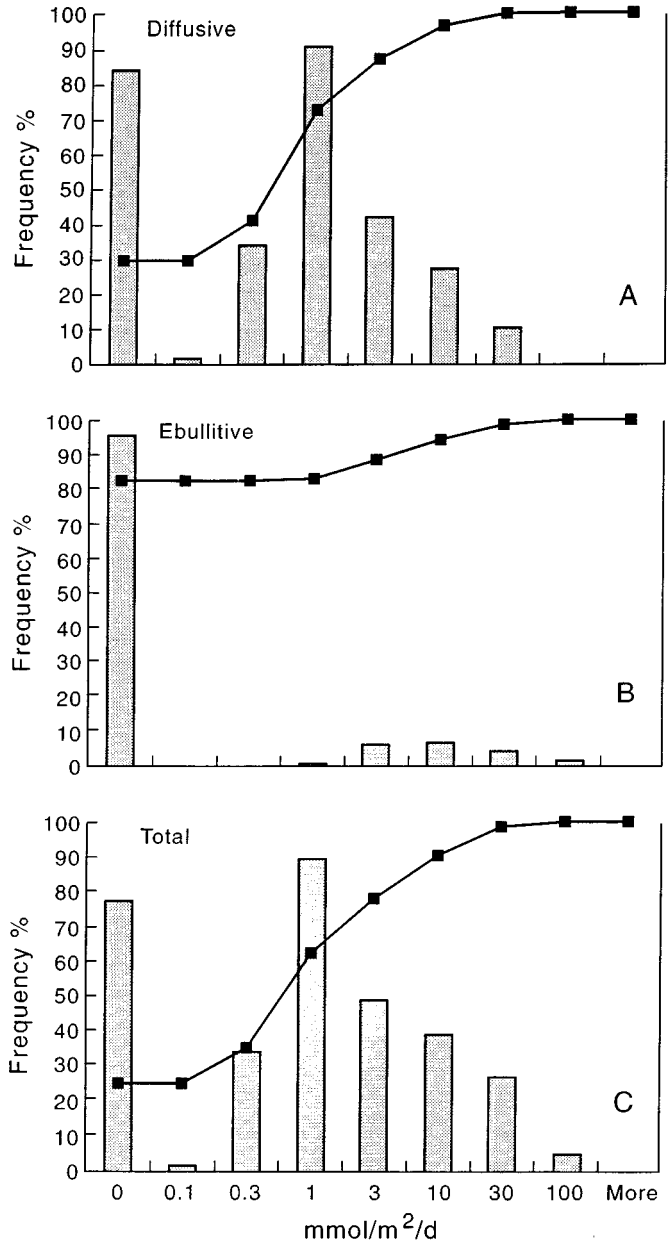

Figure 3. Frequency distribution for methane emissions from the Orinoco floodplain during 1991 and 1992. The line shows cumulative frequencies (scaled on the y-axis); the bars show relative number of samples per frequency category. Panels include diffusive flux (A), ebullitive flux (B), and total flux (C).

Table 1. Summary of methane emissions on the floodplain

	N	Percent below detection	Rate – mmol m^{-2} d^{-1}		
			Median	Mean	95th Percentile
Diffusion					
All Data	412	28	0.46	1.30	6.99
Flooded Forest	99	22	0.78	2.52	13.4
Macrophytes	102	52	0.00	0.75	1.96
Open Water	211	19	0.48	0.98	3.58
Ebullition					
All Data	412	84	0.00	1.46	9.76
Flooded Forest	99	62	0.00	4.26	30.0
Macrophytes	102	85	0.00	0.80	5.63
Open Water	211	94	0.00	0.47	1.51
Total					
All Data	412	25	0.56	2.76	13.5
Flooded Forest	99	14	1.44	6.79	36.2
Macrophytes	102	47	1.44	1.55	8.36
Open Water	211	18	0.52	1.45	6.79

most of the moderate to low rates. Figure 3 also shows the frequency distribution for ebullition. Approximately 90% of the 20-minute incubations showed no ebullition, which is reasonable given the episodic nature of ebullition. Discounting the zero values, ebullition rates are distributed in a log-normal fashion.

Table 1 summarizes some properties of the frequency distributions for ebullition and diffusion. Most measurements show diffusive emissions well above zero, but no ebullition. The mean rates for the two processes are quite similar, however, because emission rates are high whenever ebullition occurs. The 95th percentile for ebullition is about 50% higher than the 95th percentile for diffusion.

Floodplain waters

Table 1 gives statistical summaries of emission rates from flooded forest, macrophyte mats, and open water. The table combines data from the waters

Table 2. Seasonal differences in mean rates of methane emission per unit area (number of measurements is shown in parentheses)

Habitat type	Emission – mmol m^{-2} d^{-1} (N)	
	Inundation season	Isolation season
Forest		
Diffusion	2.44	3.41
Ebullition	4.26	4.24
Total*	6.70 (90)	7.65 (9)
Macrophytes		
Diffusion	0.36	1.10
Ebullition	0.81	0.80
Total*	1.17 (48)	1.90 (54)
Open Water		
Diffusion	0.94	1.05
Ebullition	0.29	0.72
Total*	1.23 (125)	1.77 (86)

*Total emissions differ seasonally at $p < 0.05$.

of the fringing floodplain with the less extensive data from waters of the delta ($N = 18$) because the two data sets are statistically indistinguishable.

Ebullition, diffusion, and total emissions for the three types of flooded habitats were compared pair-wise by habitat with the Kolmogorov-Smirnov test for differences in frequency distributions. All pair-wise combinations of habitat show highly significant differences ($p \leq 0.01$). Flooded forest has much higher diffusive emissions than macrophyte mats or open water. The diffusive emissions from macrophyte mats and open water are quite similar, even though the small difference between them is significant statistically. Ebullition rates are also highest for flooded forest. Rates of ebullition for macrophyte mats and open water are lower and are similar to each other. Emission rates combining both ebullition and diffusion are almost identical for macrophytes and open water, and are 4–5 times higher for flooded forest.

Temporal variation of methane emission is likely for the Orinoco floodplain, given the drastic change in water level between the periods of inundation and isolation. Two aspects of temporal variation must be considered: (1) emission rates per unit area for a given habitat type, and (2) areal extent of the floodplain and of each aquatic habitat within it. Rates per unit area will

Table 3. Environmental variables corresponding to measurements of methane emissions from aquatic habitats of the Orinoco floodplain. Values of the Spearman rank correlation coefficients (r_s) are shown for total flux as well as for diffusive and ebullitive fluxes. Top = water sampled near the top of the water column; bottom = water sampled just above the bottom of the water column

Variable	*N*	Mean	Percentile			r_s	
			5^{th}	Median	95^{th}	Total	(diffusive, ebullitive)
Depth, m	204	2.99	0.3	2.27	7.50	0.05	(0.06,–0.02)
Temperature, °C	205	29.1	26.3	29.0	31.8	0.03	(–0.03,0.07)
Oxygen Top, mg/L	205	5.36	2.17	5.55	8.40	–0.12*	(–0.09*,–0.10*)
Oxygen Bottom, mg/L	136	3.00	0.10	2.60	7.42	–0.15*	(–0.09*,0.15*)
Sediment C,%	75	3.13	0.95	1.90	8.37	0.23*	(0.06,0.30*)
Sediment N,%	69	0.21	0.06	0.16	0.46	0.17	(–0.04,0.27*)
CH_4 Top, μM	200	0.34	0.10	0.18	1.35	0.31*	(0.31*,0.07)
CH_4 Bottom, μM	84	1.30	0.09	0.20	2.17	0.06	(0.06,–0.02)

* $p < 0.05$.

be considered in this section; seasonal changes in area of habitat type will be considered in the calculation of total annual emissions from the floodplain.

Table 2 summarizes the seasonal differences in diffusive flux, ebullition, and total emission of methane per unit area across the three habitats of the floodplain. For the floodplain forest, diffusive emissions are higher during the isolation season, whereas ebullition is constant across seasons. The seasonal comparisons here are of minimal significance for total floodplain emissions, however, because there is very little flooded forest during the isolation season.

Macrophyte mats also show higher diffusive fluxes during the isolation season, but nearly identical ebullitive fluxes across seasons. In contrast, for open water diffusion is essentially constant across seasons, but ebullition is much higher during isolation than during inundation.

Table 3 summarizes the information on environmental variables most likely to have some causal connection with methane flux from floodplain waters. The table also indicates the results of correlation tests between each variable and the diffusive, ebullitive, and total fluxes of methane. The correlations are weak ($r_s < 0.35$ in all cases), although some are statistically significant. The amount of diffusive flux is positively correlated with the amount of methane dissolved in the upper water column, as would be expected; ebullitive flux is not. Both carbon and nitrogen content of sediment show a weak positive relationship to methane emission, most of which is attributable to a positive relationship between ebullition and carbon. Oxygen at either

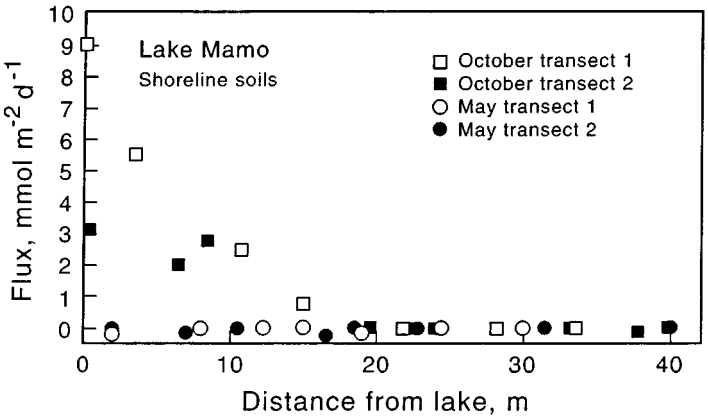

Figure 4. Emission of methane form soils on the Orinoco floodplain near Lake Mamo during the drainage phase (October) and the isolation phase (May). The x-axis shows distance from the water's edge.

the top or bottom of the water column shows a weak ($r_s < 0.20$) but significant negative correlation with methane emission, due mainly to ebullition.

For dissolved oxygen, correlation analysis might fail to detect a relationship that could be expressed best as a step function of oxygen concentration, i.e., oxygen might have no relationship to methane emissions except at the lowest oxygen concentrations. This problem was approached through a nonparametric comparison of means (Fisher exact probability test) for emission rates corresponding to two sets of oxygen conditions for the bottom of the water column: above the median (2.6 mg L^{-1}) and below the median. The test indicates a significant difference ($p < 0.05$) between the emission rates of low-oxygen and high-oxygen conditions for diffusive, ebullitive, and total fluxes. Total emissions are 56% higher when oxygen concentration near the bottom is below the median (corresponding mainly to the inundation season).

Exposed soils of the Orinoco River floodplain

The studies of floodplain soils at Lake Mamo (fixed transects) show the effect of proximity to the water's edge during drainage and the effect of desiccation during isolation (Figure 4). During October (drainage phase of the inundation season), emission rates were highest adjacent to the water and declined steadily to zero at a distance of about 20 m from the water. Integrated over distance, the emissions were 80 mmol d^{-1} per m of shoreline for one transect and 40 for a second transect (mean, 60 $mmol^{-1}$ m^{-1} d^{-1}). By May (isolation), the water had receded some 500 m, and emissions were nil.

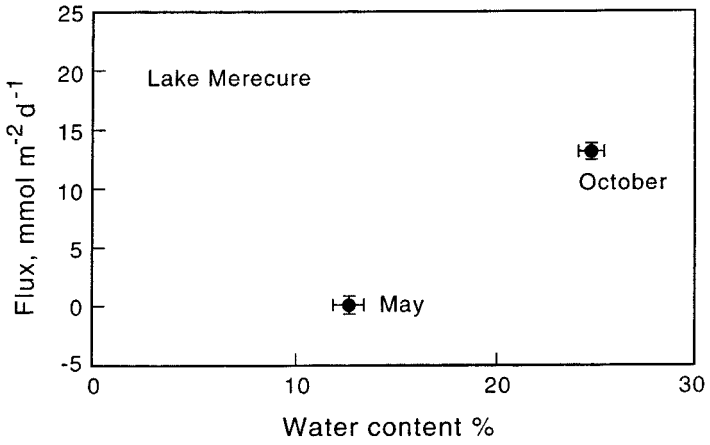

Figure 5. Emission of methane from soils of the Orinoco floodplain near Lake Merecure showing the relationship between methane emission, water content of sediment, and time of year. October falls within the drainage phase, and May falls within the isolation phase of the annual hydrologic cycle. Error bars show standard errors for means of variables on both axes.

The data for Lake Merecure (moving transects) illustrate the effect of organic matter and confirm the seasonal shift, related to soil water content, from positive to negligible methane flux that was observed at Lake Mamo (Figure 5). Lake Merecure was sampled where macrophytes were stranded along the shoreline during the period of falling water. In October, when soils 4 m from the water were moist (25% water) and were covered by decaying macrophytes, they emitted 4–6 times as much methane (Figure 5) as soils 4 m from the water at Lake Mamo, where no macrophytes were stranded (Figure 4). In May, during isolation, the soils were drier (13% water), and the fluxes were nil.

The measurements at Lake Redonda (Figure 6) verify the restriction of emissions to the drainage phase, when water content of soils is highest (all samples were taken within 20 m of the water's edge).

The sampling of floodplain soils shows that soils having a water content below approximately 25% emit no measurable amount of methane. During the drainage phase, soils within approximately 20 m of the water's edge can be expected to have a water content of 25% or more. In the absence of large amounts of organic matter (stranded macrophytes), soils near the water's edge emit approximately 60 mmol d^{-1} per m of shoreline length. Where macrophytes are stranded, the emission rates are approximately 5 times higher, as long as moisture persists. During the isolation season, there is virtually no emission of methane from floodplain soils because the soils desiccate rapidly and the rate of decline in water level is low.

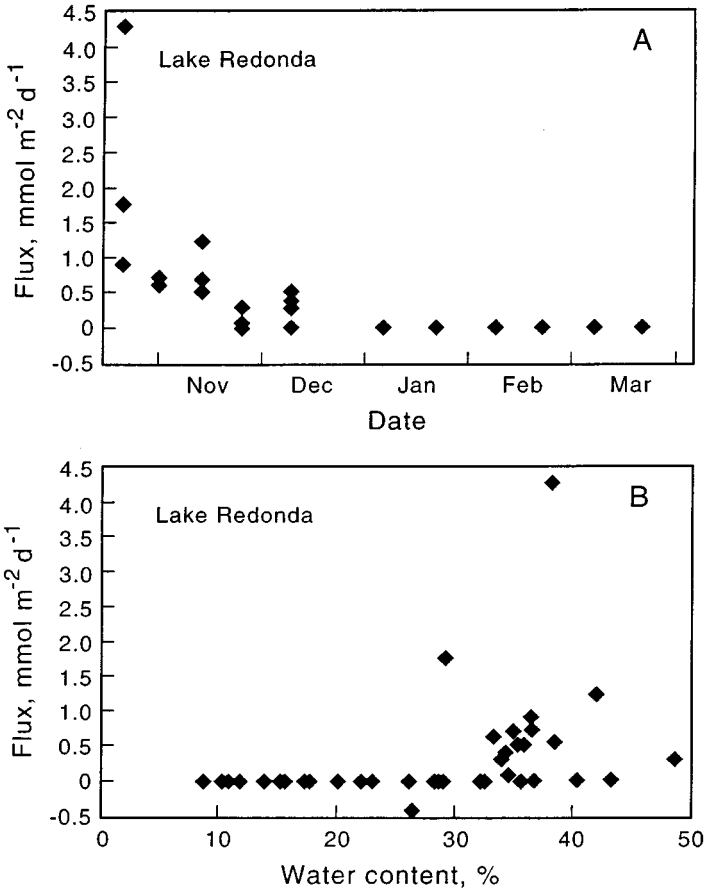

Figure 6. Emission of methane from soils near Lake Redonda on the Orinoco floodplain. Panel A shows the decline in methane emissions during the transition from the drainage phase of October and November to the isolation phase that follows. Panel B shows the relationship between water content and methane flux.

Methane in the river

Dissolved methane in the main stem of the Orinoco River near Ciudad Bolívar was measured on four dates (10 replicates per date). Variation among replicates was small (range, 0.02–0.04 μM). The means for each date were as follows (μM): 13 September, 0.16; 31 January, 0.19; 20 February, 0.16; 11 March, 0.16; mean across dates, 0.17. These concentrations are much higher than the atmospheric equilibrium concentration (0.0022 μM at 25 °C).

Total methane emission from the Orinoco River floodplain

Estimates of the seasonal changes in flooded area on the Orinoco fringing floodplain are based on field observations during 1984–1985 around Lake Tineo, near Ciudad Bolívar (Hamilton & Lewis 1987). A bathymetric map of the Tineo area, including the open water of the lake ($\sim$2 km^2) as well as the surrounding vegetated floodplain, was constructed from aerial photographs and echosounding surveys coinciding with maximum inundation. The water depth was taken from a staff gauge at the lake. The gauge reading and bathymetry were used to estimate the area of inundation at weekly or biweekly intervals between June 1984 and June 1985.

A mean annual hydrograph for the Orinoco River at Ciudad Bolívar was derived from daily stage data collected by the Venezuelan Ministerio del Ambiente y de los Recursos Naturales Renovables (unpublished reports) between 1926 and 1982. Comparison of the long-term mean hydrograph with the hydrograph for 1984–1985 shows that the river's flood cycle was not unusual during the year of hydrologic observations at Lake Tineo. The monthly area of inundation for the entire floodplain was estimated from a plot of fractional inundation area in the Lake Tineo area against river stage. The rising and falling limbs of the hydrograph were treated separately because relationships between inundation and river stage differ for these two phases.

The total area of fringing floodplain between the confluence of the Meta River and the mouth is 6960 km^2 (Hamilton & Lewis 1990a); the area of fringing floodplain upriver from this confluence is small and is not included here. Planimetric measurements from maps (1:100,000 scale) by Hamilton and Lewis (1990a) indicate that the fringing floodplain is composed of forest (79%), macrophyte mats (15%) and open water (6%) at the height of inundation. The area of open water remains nearly constant throughout the year (Hamilton & Lewis 1990a). Changes in the extent of inundated area are assumed to occur through change in the area of flooded forest and macrophyte mats, but without change in the ratio of these two types of cover.

As indicated by the comparison of seasonal emission rates, emissions must be computed separately for the isolation season (January through June) and the inundation season (the remainder of the year). In addition, emissions are calculated separately for open water, macrophyte mats, and flooded forest, each of which is weighted by the appropriate area in a given month for a year of characteristic hydrology as judged from the long-term record.

The Orinoco delta is a second major component of the total emissions. The areal extent of floodplain located within the delta that is not directly influenced by seawater was determined by electronic planimetry of a map published by van Andel (1967). This region, which is called the upper delta,

Table 4. Summary of emission rates for the Orinoco fringing floodplain and upper delta (total area, 14,500 km^2)

	Tg $CH_4 yr^{-1}$			% of Total
	Inundation	Isolation	Total	
Forest	0.138	0.025	0.163	94
Macrophytes	0.004	0.001	0.005	4
Open Water	0.002	0.002	0.004	2
Soils	0.001	0.000	0.001	0
Total	0.145	0.029	0.174	100
% of Total	83	17	100	—

lacks mangroves, which are indicative of saltwater intrusion (Pannier 1979). The total area of vegetated floodplain within the upper delta is 7500 km^2. The delta lacks open water (lakes), although it does contain distributary channels of small areal coverage (not included here). Proportions of flooded forest and macrophyte beds are about the same as for the fringing floodplain; changes in area are estimated by the same procedure as for the fringing floodplain.

The contribution of soils is estimated from the mean emission per unit length of shoreline (60 $mmol^{-1}$ m^{-1} d^{-1} where stranded macrophytes are absent and 300 $mmol^{-1}$ m^{-1} d^{-1} where stranded macrophytes are present). The percentage of shoreline with stranded macrophytes in a given month is assumed to correspond to the percent areal coverage of the floodplain by macrophytes the preceding month. The amount of shoreline is estimated from the collective perimeters of all basins on the fringing floodplain (5536 km, as determined by planimetry). The emissions apply only to the drainage phase of the annual hydrologic cycle (September, October, November), and are negligible at other times of the year.

Table 4 summarizes the methane emissions from the fringing floodplain and upper deltaic floodplain of the Orinoco (total, 0.17 Tg yr^{-1} or 7.1 mmol d^{-1} day per m^2 of water surface). The estimate does not include the extensive savanna floodplains of the Orinoco Llanos, which are contiguous with the Orinoco fringing floodplain but are hydrologically and ecologically distinct (Hamilton & Lewis 1990a). Figure 7 shows the seasonal pattern of total emissions.

Uncertainty in the emission rates was estimated by Monte Carlo methods from the frequency distributions of ebullition and diffusion plus information on the variability of replicate samples. Two thousand estimates were made of annual means based on random samples from the frequency distributions for

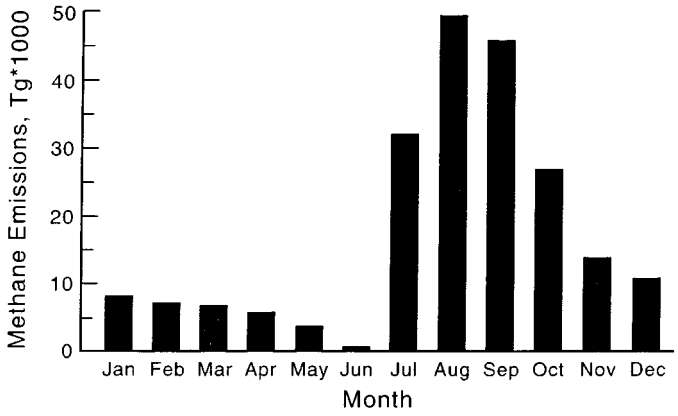

Figure 7. Seasonal pattern of total methane emission from the Orinoco floodplain.

Table 5. Stable isotope ratios (‰) of methane emitted from the Orinoco River floodplain. Data are given as mean ± s.d. (N)

	$\delta^{13}C$	δD
Flooded forest		
Inundation season	–62.2 ± 2 (10)	–271 ± 30 (8)
Isolation season	—*	—*
Macrophytes		
Inundation season	–53.5 ± 0.1 (2)	–305 ± 0.1 (2)
Isolation season	–64.4 ± 1.7 (5)	–246 ± 4 (3)
Open Water		
Inundation season	–64.1 ± 3.8 (5)	–247 (1)
Isolation Season	–66.4 ± 0.2 (3)	–259 ± 1 (2)

*Flooded forest was not present in significant amounts during the isolation season.

rates and errors in rates. The resulting frequency distribution of means is the basis for estimating uncertainty in the mean of field measurements.

The uncertainty analysis was based on variability for flooded forest because contributions of other habitats is sufficiently small that any differences in their variability would have little effect on the estimate of uncertainty in the overall mean emission rate. The uncertainty analysis indicates that the mean total emission rate per unit surface area has a standard deviation of ±18%. When the rates are summed over monthly surface areas, additional

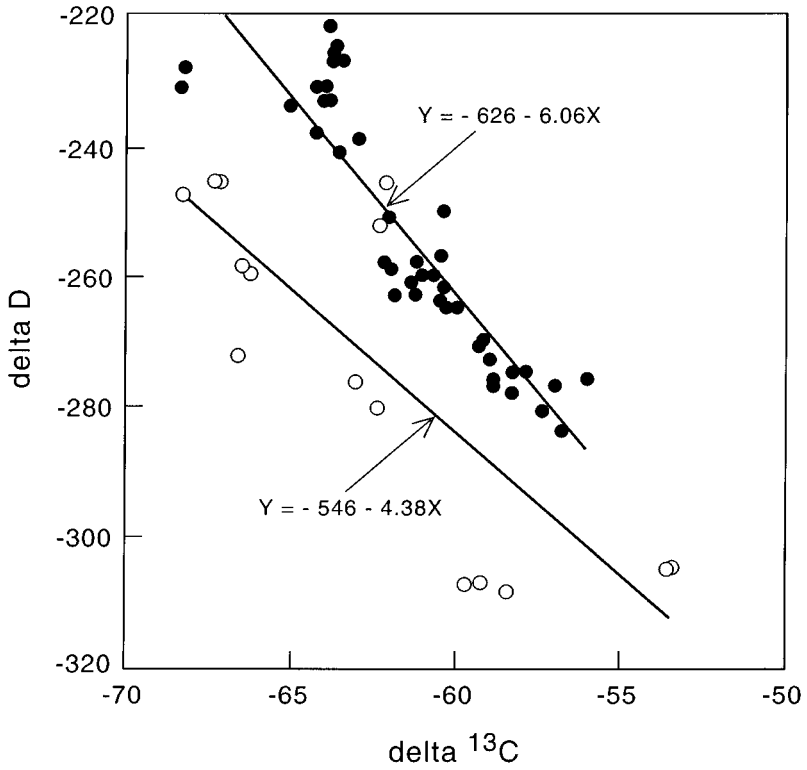

Figure 8. The relationship between $\delta^{13}C$ and δD of methane colected on the Orinoco floodplain (open circles) and the data of Burke et al. (1988a) for Cape Lookout Bight sediments (closed circles), where seasonal variation in $\delta^{13}C$ and δD were attributed to variation in methane production pathways.

error is introduced through the estimates of surface area. This source of error cannot be estimated, but is probably below 20%.

Isotopic composition of methane from the floodplain

The mean stable isotope values of methane samples collected from the principal environments of the Orinoco floodplain at high and low water ranged from –53 to –66‰ for $\delta^{13}C$ and from –247 to –305‰ for δD (Table 5). The most ^{13}C-enriched and D-depleted methane was collected from floating macrophyte mats and flooded forest during high water. The data show an inverse relationship between δD and $\delta^{13}C$ (Figure 8).

The flux-weighted mean isotopic ratios for methane emitted from the Orinoco River floodplain can be estimated from Table 5, which summarizes data collected from flux chambers and sediment bubbles. Methane collected

by the two techniques did not differ systematically in isotopic composition. The weighted average isotopic composition of methane emitted across habitats and seasons is –62 ± 8‰ for $\delta^{13}C$ and of –271 ± 27‰ for δD. Uncertainties were calculated from the propagation of errors associated with the standard deviations of measurements and the assumption of 20% uncertainty in the areal extent of floodplain habitats.

Discussion

Both ebullition and diffusion contribute significantly to total methane flux on the Orinoco floodplain; their relative contributions are similar to those observed on other tropical floodplains. Relative contributions of ebullition and diffusion differ among the three habitat types. For flooded forest, 63% of emission is accounted for by ebullition and 37% by diffusion. The relative contributions are very nearly the same for the floodplain as a whole (60% ebullition and 40% diffusion) because flooded forest accounts for 94% of total methane loss from the floodplain. For the Amazon, Devol et al. (1990) found that ebullition accounted for 73% of flux at high water and 59% at low water. In a review of Amazon data, Bartlett and Harriss (1993) reported that ebullition accounted for 20–70% of methane flux.

The relative contribution of ebullition is lower on the Orinoco floodplain for macrophytes and open water than it is for flooded forest. In macrophyte mats, the contribution of ebullition is 55%. This is slightly lower than estimates for the Amazon (Bartlett et al. 1988, 64%; Wassmann et al. 1992, 67%). For open water of the Orinoco floodplain, only about 32% of total emission is explained by ebullition. For the Amazon, the amount is closer to 50% (Chanton & Dacey 1991).

The mean flux of methane per unit of wetted area (time-weighted mean, 5200 km^2 for the fringing floodplain plus upper delta) is 7.1 mmol m^{-2} d^{-1} (114 mg $m^{-2}d^{-1}$). The mean areal emission rate of methane for the Amazon is two to three times higher (Bartlett & Harriss 1993). One especially striking comparison is for macrophyte mats, which yield over 12 mmol m^{-2} d^{-1} on the Amazon, but only about 1.6 mmol m^{-2} d^{-1} on the Orinoco.

Differences in methane yield between the Orinoco and Amazon are probably explained by physical differences in the two floodplains. The waters of the Amazon floodplain are considerably deeper, and the interval of inundation is longer than for the Orinoco (time that 50% or more of floodplain forest is inundated 3.3 months for Orinoco and 5.3 months for Amazon: S.K. Hamilton and S.J. Sippel, unpublished data). Consequently, anoxia over the sediments is commonplace on the Amazon floodplain, whereas anoxia seldom occurs on the Orinoco floodplain (Table 3); greater rates of methane

production thus would be expected for the Amazon. Consistent with this interpretation are methane concentrations near the bottom and top of the water column of the Orinoco floodplain (Table 3), which are lower than concentrations typical of the Amazon floodplain (e.g., Devol et al. 1990).

Seasonality in the emission rates for specific habitat types on the Orinoco floodplain is relatively low, even though statistically significant. Higher emissions from macrophyte mats and open water during isolation may be accounted for by the weakness of water movement at this time or by the senescence of macrophytes in response to steady decline of water level. While the mechanisms behind seasonality are of biogeochemical interest, seasonal differences affect the estimates of total annual emission very little because most of the total emission (83%) occurs during the season of inundation and originates from flooded forest that covers most of the seasonally inundated land.

Correlations of methane emission with a number of environmental variables are statistically significant but too weak to serve as a basis either for prediction or mechanistic analysis. The data suggest that the relative importance of factors governing methane flux varies both temporally and spatially.

Methane in the river exceeds saturation by almost two orders of magnitude. Data for the Amazon (Richey et al. 1988) and Pantanal region (Hamilton et al. 1997) show similar or even greater supersaturation. Presumably this methane originates largely from lateral sources of methane-rich water and persists because of slow gas exchange between the atmosphere and waters of deep rivers.

In global and regional atmospheric models of methane sources and sinks (Tyler 1986; Stevens & Engelkemeir 1988; Quay et al. 1988, 1991; Craig et al. 1988; Lowe et al. 1994), knowledge of the stable isotopic composition of methane sources can help place constraints on their contributions. While northern wetlands have received recent attention (e.g., Lansdown et al. 1992; Martens et al. 1992) there have been, with the exception of the Amazon (Devol et al. 1988, 1996), only a few studies documenting the isotopic composition of methane emitted from tropical wetlands (Tyler et al. 1988).

Methane samples collected from the Orinoco floodplain show considerable variation in isotope ratios. Factors that cause such variations include methane production (Whiticar et al. 1986) and oxidation (Coleman et al. 1981) as well as variations in the isotopic composition of the organic substrate (e.g. Chanton & Smith 1993). The relationship between δD and δ^{13}C for Orinoco methane is probably caused by spatial variation in the relative importance of the two primary mechanisms of methane production: acetate

fermentation and CO_2 reduction. Acetate fermentation produces CH_4 that is D-depleted and ^{13}C-enriched compared to methane produced via CO_2 reduction (Burke et al. 1988a, b; Martens et al. 1986, 1992; Whiticar et al. 1986; Woltemate et al. 1984). Acetate fermentation is generally associated with the formation of methane from labile organic materials (Schoell 1988; Sugimoto & Wada 1993). The greater importance of acetate fermentation in sediments of vegetated wetlands relative to unvegetated sediments has been inferred from isotopic data (Martens et al. 1992).

The slope of the line that relates δD to $\delta^{13}C$ for the Orinoco data is –4.4 (Figure 8), which is similar to the slope of –6.1 for the data of Burke et al. (1988a). Together, the two data sets suggest that the production effect causes a 5 ± 1‰ negative change in δD for each 1‰ positive change in $\delta^{13}C$. Figure 8 shows the Orinoco data alongside the Burke data because the latter is the most extensive data set reporting inverse relationships between $\delta^{13}C$ and δD of CH_4 that are attributable to production pathway effects. In laboratory experiments, methane oxidation causes a positive change in δD of 8 to 14‰ for each 1‰ positive change in $\delta^{13}C$ (Coleman et al. 1981); this ratio was between 3–5‰ for field measurements conducted by Happell et al. (1994) and Burke et al. (1988b). Sugimoto and Wada (1993, 1995) and Waldron et al. (1998) have reported results of laboratory experiments showing that shifts in methane production pathways cause shifts in the $\delta^{13}C$ of methane, but not systematic inverse variations in the δD of methane.

The Orinoco field observations (Figure 8), as well as those of Burke et al. (1988a, b) and Martens et al. (1992) for other locations, are inconsistent with the laboratory studies of Sugimoto and Wada (1995). In a study of methane release from a Texas rice paddy, however, Tyler et al. (1997) observed that δD was constant, as would be expected from the studies of Sugimoto and Wada (1995) and Waldron et al. (1998). Only additional investigation will clarify the reasons for these apparently contradictory results from different studies.

The methane emitted from the Orinoco floodplain (–62 ± 8‰ $\delta^{13}C$; –271 ± 27‰ δD) is somewhat ^{13}C-depleted relative to $\delta^{13}C$ values reported by Quay et al. (1988) for the Amazon floodplain (–53 ± 8‰). The average of a number of $\delta^{13}C$ samples collected from the Amazon floodplain by Wassmann et al. (1992) is similar to that of Quay et al. (1988). Methane from sediment gas bubbles in the Pantanal wetland of South America (S.K. Hamilton and J. Chanton, unpublished data) is similar to the Amazon in $\delta^{13}C$ (–55 ± 6‰; N = 31), but similar to the Orinoco in δD (–287 ± 14‰; N = 24). Weighting the results from the three wetlands equally yields a mean for tropical methane of –57 ± 5‰ for $\delta^{13}C$ and –299 ± 35‰ for δD. These values show enrichment of methane in ^{13}C and D relative to methane from most northern wetlands (Martens et al. 1992; Lansdown et al. 1992).

Variations in the isotopic composition of substrate may be important in explaining differences among tropical wetlands. In the Amazon River floodplain, 80–90% of the macrophytes consist of C-4 grasses (*Paspalum* and *Echinochloa*: Junk 1970; Fisher & Moline 1992). Dominant macrophytes of the Orinoco River floodplain include not only *Paspalum*, but also a C-3 plant *(Eichhornia* spp.: Hamilton & Lewis 1987), which is isotopically lighter than *Paspalum* (–28‰ versus –12‰ for δ^{13}, Hamilton et al. 1992). The Pantanal wetland supports a greater diversity of macrophytes, including C-4 species (Hamilton et al. 1995). Chanton and Smith (1993) demonstrated that sedimentary bubbles collected from beneath stands of the C-3 plant *Oryza*, which has a mean δ^{13}C of –28.3‰, contained isotopically lighter methane (δ^{13}C, –61.3 ± 0.3‰) than bubbles (δ^{13}C, –51.7 ± 0.9‰) collected from beneath the C-4 plant *Paspalum*, which has a mean δ^{13}C of –11.4‰.

Conclusion

Methane flux from the Orinoco would be grossly overestimated if emission rates per unit area for the Amazon were used in the estimate. Differences between the Amazon and the Orinoco that seem relatively small compared with the general range of variation among wetlands may cause great differences in the emission rate per unit area of the two floodplains. Most importantly, the waters of the Orinoco floodplain lack anoxia near the sediments, and the floodplain is broadly inundated for a much briefer period than the floodplain of the Amazon. Thus anoxia at the sediment surface is less likely in the Orinoco floodplain and, when it does occur, is of shorter duration than in the Amazon. The result is a smaller methane output per unit area on the Orinoco than the Amazon.

One weak link in the estimation of regional methane emissions from tropical wetlands has been the areal extent of flooding (Bartlett et al. 1990; Devol et al. 1990). The application of Scanning Multichannel Microwave Radiometer (SMMR) technology is promising for this endeavor (Sippel et al. 1994, 1998; Hamilton et al. 1996). A 9-year record of SMMR observation indicates that the water surface area on the Amazon floodplain averages 45,900 km^2 (Sippel et al. 1998). The correspondence between river stage height and water surface area (the same approach used here for the Orinoco floodplain) allowed Sippel et al. (1998) to extend their estimate to the past 94 years (46,800 km^2). In light of this information, it is likely that the floodplain areas used by Bartlett et al. (1990) and Devol et al. (1990) to extrapolate their emission rates are too large. Given an area of 46,800 km^2 for the Amazon floodplain, the same extrapolation methods employed by Bartlett et al. (1990) and Devol et al. (1990), yield a revised estimate of 1–2 Tg yr^{-1} methane

emission from the Amazon, as compared to the original estimate of 2–14 Tg yr^{-1}. A combination of the emission estimate from the Orinoco floodplain (0.2 Tg yr^{-1}) with the revised emission estimate for the Amazon suggests that tropical wetlands are not as large a methane source as indicated by Bartlett and Harris (1993). In general, estimates of methane emissions from wetlands to the atmosphere are being revised downward as more information becomes available (Moore et al. 1994). Other sources of methane appear to be greater than previously believed.

Acknowledgements

This paper is dedicated to the late Dr. Enrique Vásquez; without whom this project would have been much more difficult. We thank the Fundación La Salle de Ciencias Naturales for logistical support. R. Striegl of the USGS National Research Program and the USGS Global Change Hydrology Program provided technical support. M. Boeder, D. Naiman, R. Armas, and L. Blanco helped in the field. This work was supported by grant number NAGOAA-D-AC823 to WML and LKS from the Global Change Program of the U.S. National Oceanographic and Atmospheric Administration and by grant number NAGW-3855 to JPC from the Terrestrial Ecology Program of the U.S. National Aeronautics and Space Administration.

References

Bartlett KB, Crill PM, Sebacher DI, Harriss RC, Wilson JO & Melack JM (1988) Methane flux from Central Amazonian floodplain. J. Geophys. Res. 93: 1573–1582

Bartlett KB, Crill PM, Bonassi JA, Richey JE & Harriss RC (1990) Methane flux from the Amazon River floodplain: Emissions during rising water. J. Geophys. Res. 95: 16773–1678

Bartlett KB & Harriss RC (1993) Review and assessment of methane emissions from wetlands. Chemosphere 26: 261–320

Burke RA, Martens CS, & Sackett W (1988a) Seasonal variations of D/H and $^{13}C/^{12}C$ ratios of microbial methane in surface sediments. Nature 332: 829–831

Burke RA, Barber T & Sackett W (1988b) Methane flux and stable H and C isotope composition of the sedimentary methane from the Florida Everglades. Global Biogeochem. Cycles 2: 329–340

Chanton JP & Dacey JWH (1991) Effects of vegetation on methane flux, reservoirs, and carbon isotopic composition. In: Sharkey TD, Holland EA & HA Mooney (Eds) Trace Gas Emissions by Plants (pp 65–91). Academic Press

Chanton JP, Whiting GJ, Showers W & Crill PM (1992a) Methane flux from *Peltandra virginica* – stable isotope tracing and chamber effects. Global Biogeochemical Cycles 6: 15–33

Chanton JP, Martens CS, Kelley CA, Crill PM and Showers WJ (1992b) Methane transport mechanisms and isotopic fractionation in emergent macrophytes of Alaskan tundra lakes. J. Geophys. Res. 97: 16681–16688

Chanton JP & Smith LK (1993) Seasonal variations in the isotopic composition of methane associated with aquatic emergent macrophytes of the central Amazon basin. In: Oremland RS (Ed.) The Biogeochemistry of Global Change: Radiative Trace Gases (pp 619–633). Chapman & Hall, NY

Cicerone RJ & Oremland RS (1988) Biogeochemical aspects of atmospheric methane. Global Biogeochem. Cycles 2: 299–327

Coleman DD, Risatte JB & Schoell M (1981) Fractionation of carbon and hydrogen isotopes by methane-oxidizing bacteria. Geochim. Cosmochim. Acta 45: 1033–1037

Coleman ML, Sheperd TJ, Durchman J, Rouse J & Moore G (1982) Reduction of water with zinc for hydrogen isotope analysis. Anal. Chem. 54: 993–995

Craig H, Chou CC, Wehlan JA, Stevens cm & Engelkemeir A (1988) The isotopic composition of methane in polar ice cores. Science 242: 1535–1539

Devol AH, Richey JE, Clark WA & King SL (1988) Methane emissions to the troposphere from the Amazon floodplain. J. Geophys. Res. 93: 1583–1592

Devol AH, Richey JE, Forsberg BR & Martinelli LA (1990) Seasonal dynamics in methane emissions from the Amazon River floodplain to the troposphere. J. Geophys. Res. 95: 16417–16426

Devol AH, Richey JE, King SL, Lansdown J & LA Martinelli (1996) Seasonal variations in the ^{13}C-CH_4 of Amazon floodplain waters. In: Adams DD, Seitzinger SP & Crill PM (Eds) Cycling of Reduced Gases in the Hydrosphere (pp 173–178). Internat. Verein. Theoret. Limnologie

Fisher TR & Moline MA (1992) Seasonal plant cover on the Amazon River floodplain with aerial videography and image analysis. In: Blazquez CH (Ed.) Proc. 13th Biennial Workshop on Color Aerial Photography in Plant Sciences (pp 209–216). ASPRS, Bethesda, MD

Gupta MS, Tyler S & Cicerone R (1996) Modeling atmospheric $^{13}CH_4$ and the causes of recent changes in atmospheric CH_4 amounts. J. Geophys. Res. 101: 22923–22932

Hamilton SK & Lewis WM, Jr. (1987) Causes of seasonality in the chemistry of a lake on the Orinoco River floodplain. Limnol. Oceanogr. 32: 1277–1290

Hamilton SK & Lewis WM, Jr. (1990a) Physical characteristics of the fringing floodplain of the Orinoco River, Venezuela. Interciencia 15: 491–500

Hamilton SK & Lewis WM Jr. (1990b) Basin morphology in relation to chemical ecological characteristics of lakes on the Orinoco River floodplain, Venezuela. Arch. Hydrobiol. 119: 393–425

Hamilton SK, Lewis WM Jr. & Sippel SJ (1992) Energy sources for aquatic animals in the Orinoco River floodplain: Evidence from stable isotopes. Oecologia 89: 324–330

Hamilton SK, Sippel SJ & Melack JM (1995) Oxygen depletion and carbon dioxide and methane production in waters of the Pantanal wetland of Brazil. Biogeochemistry 30: 115–141

Hamilton SK, Sippel SJ & Melack JM (1996) Inundation patterns in the Pantanal wetland of South America determined from passive microwave remote sensing. Archiv für Hydrobiologie 137: 1–23

Hamilton SK, Sippel SJ, Calheiros DF & Melack JM (1997) An anoxic event and other biogeochemical effects of the Pantanal wetland on the Paraguay River. Limnol. Oceanogr. 42: 257–272

Happell JD, Chanton JP & Showers W (1994) The influence of methane oxidation on the stable isotopic composition of methane emitted from Florida Swamp forests Geochim. Cosmochim. Acta. 58: 4377–4388

Hoefs J (1987) Stable Isotope Geochemistry. Springer

Ioffe BV & Vitenberg AG (1984) Head-space Analysis and Related Methods in Gas Chromatography. Wiley, NY.

Junk WJ (1970) Investigations on the ecology and production-biology of the "floating vegetation" and its ecology. Amazoniana 2: 449–495

Junk WJ (1997) The Central Amazon Floodplain: Ecology of a Pulsing System. Springer, Berlin

Lansdown JM, Quay PD & King SL (1992) CH_4 production via CO_2 reduction in a temperate bog: A source of ^{13}C-depleted CH_4. Geochim. Cosmochim. Acta 56: 3493–3503

Lesack LFW & Melack JM (1991) The deposition, composition, and potential sources of major ionic solutes in rain of the Central Amazon basin. Water Resources Res. 27: 2953–2977

Lewis WM Jr, Hamilton SK & Saunders JF III (1995) Rivers of Northern South America. In: Cushing C & Cummins K (Eds) Ecosystems of the World: Rivers (pp 219–256). Elsevier, NY

Lowe D, Brenninkmeijer AC, Brailsford G, Lassey K & Gomez A (1994) Concentration and ^{13}C records of atmospheric methane in New Zealand and Antarctica: Evidence for changes in methane sources. J. Geophys. Res. 99: 16913–16925

Martens CS, Blair NE, Green CD & Des Marais DJ (1986) Seasonal variations in the stable carbon isotopic signature of biogenic methane in a coastal sediment. Science 233: 1300–1303

Martens CS, Kelley CA, Chanton JP & Showers WJ (1992) Carbon and hydrogen isotopic composition of methane from wetlands and lakes of the Yukon-Kuskokwim Delta of the Alaskan tundra. J. Geophys. Res. 97: 16689–16701

Matthews E & Fung I (1987) Methane emission from natural wetlands: Global distribution, area, and environmental characteristics of sources. Global Biogeochem. Cycles 1: 61–86

McAuliffe C (1971) Gas chromatographic determination of solutes by multiple phase equilibrium. Chem. Technol. 1: 46–51

Melack JM & Fisher TR (1983) Diel Oxygen variations and their implications for Amazon floodplain lakes. Arch. Hydrobiol. 98: 422–442

Melack JM & Forsberg BR (in press) Biogeochemistry of Amazon floodplain lakes and associated wetlands. In: McClain ME and Richey JE (Eds) The Biogeochemistry of the Amazon Basin and its Role in a Changing World. Oxford

Moore TR, Heyes A & Roulet NT (1994) Methane emissions from wetlands, southern Hudson Bay lowland. J. Geophys. Res. 99: 1455–1467

Pannier F (1979) Mangroves impacted by human-induced disturbances: A case study of the Orinoco Delta mangrove ecosystem. Environ. Managt 3: 205–216

Quay PD, King SL, Landsdown JM & Wilbur D (1988) Isotopic composition of methane released from wetlands: Implications for the increase in atmospheric methane. Global Biogeochem. Cycles 2: 385–397

Quay PD, King SL, Stutsman J, Wilbur DO, Steele LP, Fung I, Gammon RH, Brown TA, Farwell, Grootes PM & Schmidt FH (1991) Carbon isotopic composition of atmospheric CH_4: Fossil and biomass burning source strengths. Global Biogeochem. Cycles 5: 25–47

Richey JE, Devol AH, Wofsy SC, Victoria R & Ribeiro MNG (1988) Biogenic gases and the oxidation and reduction of carbon in Amazon River and floodplain waters. Limnol. Oceanogr. 33: 551–561

Schoell M (1988) Multiple origins of methane in the earth. Chem. Geol. 71: 1–10

Sippel SJ, Hamilton SK & Melack JM (1994) Determination of inundation area in the Amazon River floodplain using the SMMR 37 Ghz polarization difference. Remote Sensing Environ. 48: 70–76

Sippel SJ, Hamilton SK, Melack JM & Novo EMM (1998) Passive microwave observations of inundation area and the area/stage relation in the Amazon River. Int. J. Remote Sensing 19: 3055–3074

Smith LK & Lewis WM Jr (1992) Seasonality of methane emissions from five lakes and associated wetlands of the Colorado Rockies. Global Biogeochem. Cycles 6: 323–338

Stevens CM & Engelkemeir A (1988) Stable carbon isotopic composition of methane from some natural and anthropogenic sources. J. Geophys. Res. 93: 725–733

Sugimoto A & Wada E (1993) Carbon isotopic composition of bacterial methane in a soil incubation experiment: contributions of acetate and CO_2/H_2. Geochim. Cosmochim. Acta 57: 4015–4027

Sugimoto A & Wada E (1995) Hydrogen isotopic composition of bacterial methane, CO_2 reduction, and acetate fermentation. Geochim. Cosmochim. Acta 59: 1339–1352

Tundisi JG, Forsberg BR, Devol AH, Zaret TM, Tundisi TM, Dos Santos A, Ribeiro JS & Hardy ER (1984) Mixing patterns in Amazon floodplain lakes. Hydrobiologia 49: 309–327

Tyler SC (1986) Stable carbon isotope ratios in atmospheric methane and some of its sources. J. Geophys. Res. 91: 13232–13238

Tyler SC (1991) $^{13}C/^{12}C$ ratios in atmospheric methane and some of its sources. In: Rogers JE & Whitman W (Eds) Microbial Production and Consumption of Greenhouse Gases (pp 395–409). American Society for Microbiology, Washington, DC

Tyler SC, Zimmerman PR, Cumberbatch C, Greenberg JP, Westberg C & Darlington JPEC (1988) Measurements and interpretation of $\delta^{13}C$ of methane from termites, rice paddies, and wetlands in Kenya. Global Biogeochem. Cycles 2: 341–355

Tyler SC, Bilek RS, Sass RL & Fisher FM (1997) Methane oxidation and pathways of production in a Texas paddy field deduced from measurements of flux $\delta^{13}C$ and δD of CH_4. Global Biogeochem. Cycles 11: 323–348

van Andel TjH (1967) The Orinoco Delta. J. Sedimentary Petrol. 32: 297–310

Vásquez E (1992) Temperature and dissolved oxygen in lakes of the Lower Orinoco River floodplain (Venezuela). Rev. Hydrobiol. Trop. 25: 23–33

Waldron S, Watson-Clark I, Hall AJ & Fallick AE (1998) The carbon and hydrogen stable isotope composition of bacteriogenic methane: a laboratory study using a landfill inoculum. Geomicrobiology 15: 157–160

Wassmann R, Thein UG, Whiticar MJ, Rennenberg H, Seiler W & Junk WJ (1992) Methane emissions from the Amazon floodplain: Characterization of production and transport. Global Biogeochem. Cycles 6: 3–13

Whiticar GJ, Faber G & Schoell M (1986) Biogenic methane formation in marine and freshwater environments: CO_2 reduction vs. acetate fermentation - Isotopic evidence. Geochim. Cosmochim. Acta 50: 693–709

Woltemate I, Whiticar MJ & Schoell M (1984) Carbon and hydrogen isotopic composition of bacterial methane in a shallow freshwater lake. Limnol. Oceanogr. 29: 285–292